Electronic decay of valence holes in clusters and condensed matter

Robin Santra, Jürgen Zobeley, and Lorenz S. Cederbaum
Theoretische Chemie, Physikalisch-Chemisches Institut, Universität Heidelberg, Im Neuenheimer Feld 229, D-69120 Heidelberg, Germany
(Received 15 May 2001; published 29 November 2001)

Following innervalence ionization of a cluster, the system can relax by electron emission, a phenomenon called *intermolecular Coulombic decay*. This process is characterized by an efficient energy transfer mechanism between neighboring monomers in the cluster. A theoretical description within the framework of Wigner-Weisskopf theory is developed, thus enabling a detailed analysis of the decay process. The main result of the formal treatment, a simple, approximate expression for the electronic decay width of an innervalence hole state, is applied to investigate the effect of cluster size. On the basis of extensive *ab initio* calculations, pronounced size effects are found in the concrete example of neon clusters. The decay lifetime decreases in a monotonic fashion from hundred femtoseconds in Ne_2 down to less than ten femtoseconds in Ne_{13}. Suggestions are made how to facilitate the experimental observation of *intermolecular Coulombic decay* in clusters and condensed matter.

DOI: 10.1103/PhysRevB.64.245104 PACS number(s): 73.22.−f, 79.60.−i, 33.80.Eh, 34.30.+h

I. INTRODUCTION

At sufficiently low temperatures any molecular species in the gas phase condenses to form liquid or solid matter. Typically, the interactions responsible for condensation—van der Waals forces or hydrogen bonds—can be classified as weak. With the aim of gaining insight into the properties of condensed matter systems, for many years researchers have been investing much effort in the study of atomic and molecular clusters.[1–3] On the one hand, clusters play a prominent role in the condensation process itself. On the other hand, they are amenable to detailed experimental and theoretical analysis at the microscopic level, and it is often possible to establish a causal connection between the results obtained for clusters and the properties of condensed matter.

Many experiments on clusters involve electron-spectroscopic methods. It is difficult to overestimate the importance of photoelectron spectroscopy[4] as an outstanding technique for quantitatively investigating the electronic structure of matter. Core ionization, by means of x-ray radiation, for example, can serve the purpose of element identification, since the energy needed for the removal of a core electron is characteristic of the involved atomic species. Furthermore, in strongly bound molecules and solids there is a measurable effect of the molecular environment on the energetics of the core hole. This phenomenon is known as chemical shift. In addition, as has been found only recently, interatomic response effects in small clusters can cause surprisingly strong satellite structures in the core-ionization spectrum.[5] Eventually, due to the high excitation energy, a core hole can undergo electronic decay, so-called Auger decay. Spectroscopy of the emitted Auger electron yields further information of interest.[6] Atoms in the vicinity of the core hole may induce not only chemical shifts in the kinetic energy spectrum of the Auger electron. They may even affect the Auger decay rate in an observable manner (see Ref. 7, and references therein).

In spite of all that, in weakly bound systems neither core ionization nor Auger spectroscopy are particularly sensitive to molecular environment effects. van der Waals and hydrogen bonds have hardly any influence on the properties of a core hole (see, e.g., Ref. 8 for a discussion). It is therefore natural to ask whether there are any electron-spectroscopic effects in the *valence* shell that are unique to clusters and, potentially, condensed matter, and that are *not* encountered in isolated gas-phase molecules.

Indeed, as Cederbaum and co-workers have discovered,[9,10] the answer to that question is yes. The novel process, which is called intermolecular Coulombic decay (ICD), is best illustrated by a concrete example. Consider an isolated water molecule. Ionizing its $2s$-type innervalence shell leads to a monocation that is energetically below the double ionization threshold. It can be concluded that such a water cation can dissipate its excess energy only by dissociation and/or photon emission on a time scale of picoseconds or longer. However, if a water cluster, consisting of two or more water monomers, is considered, the situation changes fundamentally: Now an innervalence hole decays by electron emission, on a time scale of the order of 10 femtoseconds. The emitted ICD electron has a kinetic energy of a few electronvolts. Subsequently the cluster undergoes fragmentation.

The key to understanding this phenomenon is the observation that in clusters the double ionization threshold is lowered compared to the isolated monomer. If a single molecule is doubly ionized, both charges are necessarily located in close proximity to one another. In clusters, however, the two holes can be spatially separated by placing each hole on a different monomer. In this way the repulsive Coulomb interaction between the two positive charges is reduced in the dicationic cluster, thereby causing a significant drop of the double ionization threshold.

The exact decay mechanism was identified by extensive *ab initio* electron propagator calculations and hole-population analysis of the computed quantum-mechanical states.[11,12] Returning to the example of water clusters, in a somewhat simplified picture ICD works as follows. A $2p$-type outervalence electron at the water molecule carrying the initial innervalence vacancy drops into this hole. Energy is released which is sufficient to eject an electron from the

outervalence shell of a *neighboring* monomer. Eventually, the repulsion between the two cationic water monomers that are generated in the electronic decay process leads to a Coulomb explosion of the cluster.

The ultrafast character of ICD and its associated energy transfer process is underlined by the results of *ab initio* calculations utilizing techniques of non-Hermitian quantum mechanics.[13,14] For example, the innervalence states of $(HF)_2^+$ decay by ICD electron emission after lifetimes between 12 and 38 fs. In $(HF)_3^+$, which possesses more intermolecular decay channels, the lifetimes were found to be even shorter than 10 fs.

ICD is a pure environment effect. Nevertheless, it is likely that only the nearest neighbors of an innervalence ionized monomer exert an appreciable influence on the electronic decay properties. (Even if that is not the case, additional coordination shells are expected to enhance, and not diminish, the effect.) Accordingly, it seems justified to regard small clusters as subunits of extended matter systems, and to conclude that the ICD phenomenon discovered in clusters should also be observable in condensed matter. ICD might add a new dimension to the class of electron-spectroscopic techniques that are widely applied to the investigation of surfaces. ICD offers two probes of surface properties, the ICD electrons and the Coulomb explosion fragments, both of which can escape from surfaces. In this context it is interesting to note that the kinetic energy spectra of the ICD electrons as well as of the Coulomb explosion fragments directly reflect the structure of the quantum-mechanical *wave function* (or, more accurately, its modulus squared) corresponding to the relative vibrational motion of the monomers involved in the ICD process.[15] There exists, as far as we know, no other method that can give that kind of information in a comparably pronounced fashion.

The purpose of the present paper is threefold. First, in Sec. II we provide a formal treatment of ICD, which helps elucidate the nature of the electronic decay mechanism. Second, in Sec. III a simple expression for the electronic decay rate, derived in Sec. II, is applied to cationic clusters of different sizes. This allows us to systematically investigate the influence by the environment of the monomer initially ionized. Finally, in view of the expected experimental difficulties in distinguishing ICD electrons from electrons stemming from other processes, suggestions are made in Sec. IV how these complications might be overcome.

II. CONCEPTUAL ASPECTS OF INTERMOLECULAR COULOMBIC DECAY

A. Elementary description of many-particle systems

Earlier theoretical work by Sawatzky explained the quasiatomic character of Auger spectra in narrow-band metals.[16] The two final-state holes are localized to the atom with the initial core hole, if the bandwidth is small in comparison to the Coulomb energy of a pair of localized electrons. Owing to the high kinetic energy of the emitted Auger electron, the one-center approximation for calculating Auger decay is justified and interatomic effects are relatively small. Thomas and Weightman performed a similar investigation on core holes in molecules,[17] with analogous conclusions. Here, we consider a system consisting of van der Waals or hydrogen-bonded atoms or molecules and elucidate the fate of an innervalence hole in that system. Such a hole decays via a purely intermolecular mechanism.

We adopt a tight-binding point of view and assume for clarity that the positions of the atomic nuclei are fixed in coordinate space at a local minimum of the potential energy hypersurface of the system. The description of the electrons is facilitated within the framework of the Hartree-Fock quasiparticle picture.[18,19] The eigenstates $|\varphi_p\rangle$ of the corresponding one-particle operator $\hat{F}$, the so-called Fock operator, form an orthonormal basis of the one-electron Hilbert space

$$\hat{F}|\varphi_p\rangle=\varepsilon_p|\varphi_p\rangle, \quad \langle\varphi_p|\varphi_q\rangle=\delta_{pq}, \quad \sum_p |\varphi_p\rangle\langle\varphi_p|=\mathbb{1}. \tag{1}$$

The $|\varphi_p\rangle$ in accordance with custom are referred to as spin orbitals or, simply, orbitals, the eigenvalues ε_p are orbital energies. The Hamilton operator $\hat{H}$ is then given by

$$\begin{aligned}\hat{H}&=\hat{F}+\hat{V}-\hat{V}^{(\mathrm{HF})}+V_{NN}\\&=\sum_p \varepsilon_p c_p^\dagger c_p+\frac{1}{2}\sum_{pqrs} V_{pqrs}c_p^\dagger c_q^\dagger c_s c_r\\&\quad-\sum_{pq} V_{pq}^{(\mathrm{HF})}c_p^\dagger c_q+V_{NN},\end{aligned} \tag{2}$$

where use has been made of the powerful formalism of second quantization[20] developed in quantum field theory. The operator $c_p^\dagger$ creates a (quasi)particle in the orbital $|\varphi_p\rangle$, i.e., $c_p^\dagger|0\rangle=|\varphi_p\rangle$, $|0\rangle$ denoting the vacuum state without any electrons. c_p is the corresponding annihilator $c_p|\varphi_p\rangle=|0\rangle$. The fermion field is quantized by means of the anticommutation relations

$$\{c_p,c_q\}=0, \quad \{c_p,c_q^\dagger\}=\delta_{pq}, \quad \{c_p^\dagger,c_q^\dagger\}=0, \tag{3}$$

which underlie the well known Pauli exclusion principle.

The orbital energies

$$\varepsilon_p=\int \varphi_p^\dagger(\boldsymbol{x})\left\{-\frac{\hbar^2}{2m}\boldsymbol{\nabla}^2-\sum_K \frac{Z_K e^2}{|\boldsymbol{x}-\boldsymbol{R}_K|}\right\}\varphi_p(\boldsymbol{x})d^3x+V_{pp}^{(\mathrm{HF})} \tag{4}$$

are determined by the motion of the Hartree-Fock particle in the field of the atomic nuclei of charge $Z_K e$ $(e>0)$ at spatial position $\boldsymbol{R}_K$, and its interaction $V_{pp}^{(\mathrm{HF})}$ with the effective charge cloud that comprises the other Hartree-Fock particles of the system under consideration. Note that the $\varphi_p(\boldsymbol{x})$ are two-component spinors.[21] Following a widely adopted convention we use indices $i,j,k,l,\ldots$, for orbitals which are occupied in the N-electron Hartree-Fock ground state $|\Phi_0^N\rangle := \Pi_{i=1}^N c_i^\dagger|0\rangle$. Occupied orbitals are also known as hole states. Unoccupied orbitals, or particle states, are symbolized by indices $a,b,c,d,\ldots$, whereas for general orbitals indices $p,q,r,s,\ldots$ are employed. In this fashion the general expression for the Hartree-Fock mean field reads

$$V_{pq}^{(\mathrm{HF})}=\sum_i V_{pi[qi]}. \tag{5}$$

Here we made use of the definition $V_{pq[rs]}:=V_{pqrs}-V_{pqsr}$. $V_{pq[rs]}$ consists of a direct and an exchange interaction term, depending on the electron-electron Coulomb matrix element

$$V_{pqrs}=\int\int \varphi_p^\dagger(\boldsymbol{x}_1)\varphi_r(\boldsymbol{x}_1)\frac{e^2}{|\boldsymbol{x}_1-\boldsymbol{x}_2|}\varphi_q^\dagger(\boldsymbol{x}_2)\varphi_s(\boldsymbol{x}_2)d^3x_1d^3x_2. \tag{6}$$

The nuclear repulsion energy

$$V_{NN}=\sum_K\sum_{K'<K}\frac{Z_KZ_{K'}e^2}{|\boldsymbol{R}_K-\boldsymbol{R}_{K'}|} \tag{7}$$

is a constant in the clamped-nuclei approximation. V_{NN} has no influence on the dynamics of the electrons. It is therefore disregarded subsequently.

B. Valence ionization and electron correlation

Let us assume for the moment that the Hamiltonian $\hat{H}$ is equal to the Fock operator $\hat{F}$. Then $|\Phi_0^N\rangle$ is an eigenstate of $\hat{H}$:

$$\hat{H}|\Phi_0^N\rangle=\hat{F}|\Phi_0^N\rangle=\sum_{j=1}^N \varepsilon_j|\Phi_0^N\rangle. \tag{8}$$

In this picture an ionization process corresponds to removing an electron from an occupied one-particle state, say, $|\varphi_i\rangle$. Thereby a one-hole state $c_i|\Phi_0^N\rangle$ is generated. This state is also an eigenstate of $\hat{H}$:

$$\hat{H}c_i|\Phi_0^N\rangle=\hat{F}c_i|\Phi_0^N\rangle=\sum_{j\neq i}\varepsilon_jc_i|\Phi_0^N\rangle. \tag{9}$$

It can be concluded that the ionization potential, that is, the energy difference between $c_i|\Phi_0^N\rangle$ and $|\Phi_0^N\rangle$, is $-\varepsilon_i$, the negative orbital energy of the one-particle state $|\varphi_i\rangle$.

The remarkable aspect of this result is that it still holds if the perturbation $\hat{H}_I:=\hat{V}-\hat{V}^{(\mathrm{HF})}$ is taken into account in first order ($\hat{H}=\hat{F}+\hat{H}_I$):

$$\langle\Phi_0^N|c_i^\dagger\hat{H}c_i|\Phi_0^N\rangle-\langle\Phi_0^N|\hat{H}|\Phi_0^N\rangle=-\varepsilon_i, \tag{10}$$

because $\langle\Phi_0^N|c_i^\dagger\hat{H}_Ic_i|\Phi_0^N\rangle=\langle\Phi_0^N|\hat{H}_I|\Phi_0^N\rangle$ due to the special properties of the Hartree-Fock mean field. Equation (10) is the formal foundation of Koopmans' theorem,[22] which establishes a one-to-one correspondence between energies of occupied orbitals and ionization potentials. This concept is very useful for the interpretation of experimental data. For ionization in the outervalence regime the Hartree-Fock model often yields a qualitatively correct picture. There it is usually possible to associate each ionization spectral line with the removal of an electron from a corresponding outervalence orbital.

Nevertheless, it has been shown[23] that, particularly in the innervalence region, neglect of $\hat{H}_I$ beyond first-order perturbation theory can fail severely. Under such circumstances the perturbation leads not merely to shifted ionization lines, but to a much larger number of states than expected on the basis of an effective one-particle model. This phenomenon, a striking manifestation of electron correlation, is known as breakdown of the one-particle picture.[23] Its physical foundation is strong configuration interaction of a one-hole state $c_i|\Phi_0^N\rangle$ with two-hole one-particle states $c_a^\dagger c_kc_l|\Phi_0^N\rangle$ that are close in energy, i.e., $\varepsilon_i\approx\varepsilon_k+\varepsilon_l-\varepsilon_a$. In clusters and condensed matter the number of excited two-hole one-particle configurations which couple to a given one-hole state is greatly increased in comparison to small molecular monomers, mainly because of the possibility to distribute the two holes across more than a single molecule. Therefore, electron correlation plays a particularly pronounced role in the description of excitation processes in extended matter systems. ICD, a decay mode not accessible to small, isolated molecules, is a dramatic example of such an intermolecular correlation phenomenon.

C. ICD in the framework of Wigner-Weisskopf theory

Wigner and Weisskopf[24] were the first to provide a quantum-mechanical description of decay processes. A general treatment of their method, which is based on time-dependent perturbation theory, can be found in Ref. 21, for example. In order to investigate the nature of ICD at a fundamental level, we use a suitably adapted version of Wigner-Weisskopf theory.

The term *decay* refers to the interaction of a specific discrete state with a continuum of states. The associated transition to the continuum is irreversible. Supposing that a decaying innervalence hole state can be approximated by a one-hole state $|\Phi_I^{N-1}\rangle=c_{\mathrm{iv}}|\Phi_0^N\rangle$, then a convenient choice for an orthonormal basis in the $(N-1)$-electron space is

$$\{|\Phi_J^{N-1}\rangle\}:=\{c_i|\Phi_0^N\rangle,c_a^\dagger c_kc_l|\Phi_0^N\rangle\ (k<l),c_a^\dagger c_b^\dagger c_kc_lc_m|\Phi_0^N\rangle\ (a<b,k<l<m),\ldots\}, \tag{11}$$

which consists of all one-hole, two-hole one-particle, three-hole two-particle, . . . , excitations of the N-electron Hartree-Fock ground state. The projection $\hat{H}^{(N-1)}$ of the Hamilton operator $\hat{H}$ onto this basis is partitioned into a diagonal part $\hat{H}_0^{(N-1)}$ and an off-diagonal part $\hat{H}_1^{(N-1)}$:

$$\hat{H}^{(N-1)}=\hat{H}_0^{(N-1)}+\hat{H}_1^{(N-1)}, \tag{12}$$

$$\hat{H}_0^{(N-1)}=\sum_J\langle\Phi_J^{N-1}|\hat{H}|\Phi_J^{N-1}\rangle|\Phi_J^{N-1}\rangle\langle\Phi_J^{N-1}|,$$

$$\hat{H}_1^{(N-1)}=\sum_J\sum_{K\neq J}\langle\Phi_J^{N-1}|\hat{H}|\Phi_K^{N-1}\rangle|\Phi_J^{N-1}\rangle\langle\Phi_K^{N-1}|.$$

The basis vectors $|\Phi_J^{N-1}\rangle$ are eigenvectors of $\hat{H}_0^{(N-1)}$, i.e.,

$$\hat{H}_0^{(N-1)}|\Phi_J^{N-1}\rangle=\langle\Phi_J^{N-1}|\hat{H}|\Phi_J^{N-1}\rangle|\Phi_J^{N-1}\rangle. \tag{13}$$

Without electron correlation each of these states would be stationary. The electronic decay of the initial state $|\Phi_I^{N-1}\rangle$, a

discrete eigenvector of $\hat{H}_0^{(N-1)}$ embedded with respect to energy in a continuum of other eigenstates $|\Phi_F^{N-1}\rangle$, is induced by the presence of $\hat{H}_1^{(N-1)}$. The resonance state, which results from the interaction of the discrete state with the continuum, is characterized by a *complex* energy

$$E_{\mathrm{Res}}=\langle\Phi_I^{N-1}|\hat{H}|\Phi_I^{N-1}\rangle+\Delta_I-i\Gamma_I/2. \tag{14}$$

Δ_I is the energy shift and Γ_I is the decay width of the resonance. The probability $P_I(t)$ that the system is in state $|\Phi_I^{N-1}\rangle$ at time t decreases exponentially,

$$P_I(t)=P_I(0)\exp(-t/\tau_I),\tau_I=\hbar/\Gamma_I. \tag{15}$$

The first nonvanishing perturbative contribution to Γ_I is given by the following equation:

$$\Gamma_I=2\pi\sum_{F\neq I}|\langle\Phi_F^{N-1}|\hat{H}|\Phi_I^{N-1}\rangle|^2\delta(\langle\Phi_F^{N-1}|\hat{H}|\Phi_F^{N-1}\rangle - \langle\Phi_I^{N-1}|\hat{H}|\Phi_I^{N-1}\rangle). \tag{16}$$

An innervalence hole state $|\Phi_I^{N-1}\rangle=c_{\mathrm{iv}}|\Phi_0^N\rangle$ which lies above the double ionization threshold can decay by emission of an electron in one-electron state $|\varphi_{\boldsymbol{k}}\rangle$ with continuous index $\boldsymbol{k}$ (since $|\varphi_{\boldsymbol{k}}\rangle$ is not square integrable, it is, strictly speaking, not an element of the one-electron Hilbert space). The electronic relaxation process is accompanied by the formation of two outervalence holes, one in orbital $|\varphi_{\mathrm{ov}_1}\rangle$ and one in orbital $|\varphi_{\mathrm{ov}_2}\rangle$. Therefore, the possible final states are given by $|\Phi_F^{N-1}\rangle=c_{\boldsymbol{k}}^\dagger c_{\mathrm{ov}_1}c_{\mathrm{ov}_2}|\Phi_0^N\rangle$. Other states $|\Phi_F^{N-1}\rangle$ with coupling matrix elements $\langle\Phi_F^{N-1}|\hat{H}|\Phi_I^{N-1}\rangle$ different from zero do not contribute to Γ_I, owing to the restriction imposed on their energy $\langle\Phi_F^{N-1}|\hat{H}|\Phi_F^{N-1}\rangle$ by the δ function in Eq. (16). This argument applies, on the one hand, to two-hole one-particle states with holes in orbitals other than outervalence one-particle states and, on the other hand, to three-hole two-particle states of type $c_a^\dagger c_b^\dagger c_k c_l c_{\mathrm{iv}}|\Phi_0^N\rangle$, which are the only remaining basis vectors that can couple directly to $c_{\mathrm{iv}}|\Phi_0^N\rangle$. Hence, using Eq. (2) for the Hamiltonian, the properties of the creation and annihilation operators [Eq. (3)] and Eq. (5) for the Hartree-Fock mean field, a very simple, approximate expression for the electronic decay width Γ_{iv} of a cationic innervalence resonance can be derived from Eq. (16):

$$\Gamma_{\mathrm{iv}}=2\pi\sum_{\boldsymbol{k}}\sum_{\mathrm{ov}_1}\sum_{\mathrm{ov}_2>\mathrm{ov}_1}|V_{\mathrm{ov}_1,\mathrm{ov}_2[\mathrm{iv},\boldsymbol{k}]}|^2\delta(\varepsilon_{\mathrm{iv}}-\varepsilon_{\mathrm{ov}_1}-\varepsilon_{\mathrm{ov}_2} + V_{\mathrm{ov}_1,\mathrm{ov}_2[\mathrm{ov}_1,\mathrm{ov}_2]}+\varepsilon_{\boldsymbol{k}}-V_{\boldsymbol{k},\mathrm{ov}_1[\boldsymbol{k},\mathrm{ov}_1]}-V_{\boldsymbol{k},\mathrm{ov}_2[\boldsymbol{k},\mathrm{ov}_2]}). \tag{17}$$

Let us analyze this expression. The δ function specifies the decay channels that are available for an innervalence hole created at an ionization potential of $-\varepsilon_{\mathrm{iv}}$. At the adopted level of approximation the energy of a dicationic state with holes in $|\varphi_{\mathrm{ov}_1}\rangle$ and $|\varphi_{\mathrm{ov}_2}\rangle$ is given by the sum of the individual ionization potentials of the two outervalence holes and the Coulomb interaction between them, $-\varepsilon_{\mathrm{ov}_1}-\varepsilon_{\mathrm{ov}_2}+V_{\mathrm{ov}_1,\mathrm{ov}_2[\mathrm{ov}_1,\mathrm{ov}_2]}$. The energetic accessibility of an electronic decay mode in cationic innervalence states relies on the possibility of reducing the hole-hole repulsion in the final states. In small, isolated molecules, both holes are rather close to one another. Coulomb repulsion between these holes is usually so strong that all dicationic states in small molecules are higher in energy than any monocationic innervalence state. By contrast, the double ionization threshold of clusters[25] and solids[26] is lowered due to the spatial separability of the two-hole charges, thus opening the electronic decay channels distinguishing ICD: $|\varphi_{\mathrm{ov}_1}\rangle$ and $|\varphi_{\mathrm{ov}_2}\rangle$ are localized each at a different monomer. The term $\varepsilon_{\boldsymbol{k}}-V_{\boldsymbol{k},\mathrm{ov}_1[\boldsymbol{k},\mathrm{ov}_1]}-V_{\boldsymbol{k},\mathrm{ov}_2[\boldsymbol{k},\mathrm{ov}_2]}$ in Eq. (17) describes the energy of the emitted decay electron including its residual interaction with the two holes.

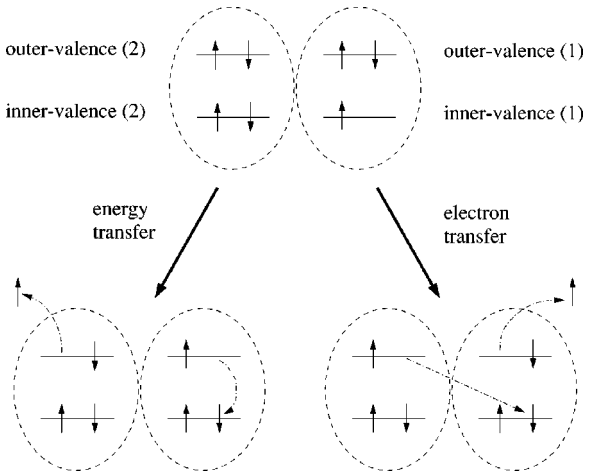

FIG. 1. Two different physical mechanisms can be identified in the theoretical description of electronic decay processes in weakly bound clusters. The mechanisms are associated with the direct and the exchange term, respectively, of the coupling matrix element $V_{\mathrm{ov}_1,\mathrm{ov}_2[\mathrm{iv},\mathbf{k}]}=V_{\mathrm{ov}_1,\mathrm{ov}_2,\mathrm{iv},\mathbf{k}}-V_{\mathrm{ov}_1,\mathrm{ov}_2,\mathbf{k},\mathrm{iv}}$ in Eq. (17). ICD of innervalence holes is best understood in terms of energy transfer between the involved monomers ($V_{\mathrm{ov}_1,,\mathrm{ov}_2,\mathrm{iv},\mathbf{k}}$). Electron transfer ($V_{\mathrm{ov}_1,\mathrm{ov}_2,\mathbf{k},\mathrm{iv}}$) is only of minor importance. Please note that both possible decay mechanisms are purely intermolecular (the two dashed ovals symbolize two neighboring monomers).

Having established the nature of the decay channels, we turn our attention to the coupling matrix elements $V_{\mathrm{ov}_1,\mathrm{ov}_2[\mathrm{iv},\boldsymbol{k}]}=V_{\mathrm{ov}_1,\mathrm{ov}_2,\mathrm{iv},\boldsymbol{k}}-V_{\mathrm{ov}_1,\mathrm{ov}_2,\boldsymbol{k},\mathrm{iv}}$. These significantly contribute to Γ_{iv} only if one of the outervalence holes, say, $|\varphi_{\mathrm{ov}_1}\rangle$, resides at the site of the initial innervalence hole, and the other outervalence hole $|\varphi_{\mathrm{ov}_2}\rangle$ is located at a neighboring monomer. Two different physical processes are described by the direct term $V_{\mathrm{ov}_1,\mathrm{ov}_2,\mathrm{iv},\boldsymbol{k}}$ and the exchange term $V_{\mathrm{ov}_1,\mathrm{ov}_2,\boldsymbol{k},\mathrm{iv}}$, as illustrated in Fig. 1. The impact of the direct term $V_{\mathrm{ov}_1,\mathrm{ov}_2,\mathrm{iv},\boldsymbol{k}}$ can be interpreted in the following manner. An electron in $|\varphi_{\mathrm{ov}_1}\rangle$ drops into the hole in $|\varphi_{\mathrm{iv}}\rangle$. The re-

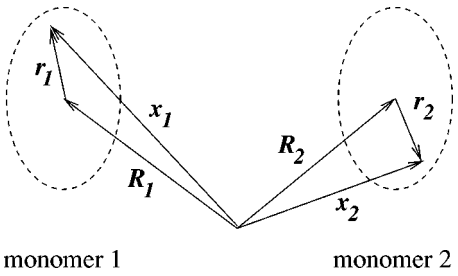

FIG. 2. Position vectors employed to derive the long-range behavior of the intermolecular Coulombic decay rate. $\boldsymbol{R}_1$ and $\boldsymbol{R}_2$ denote the centers of mass of the monomers participating in the decay process. $\boldsymbol{r}_i$ $(i=1,2)$ is the position of electron i with respect to $\boldsymbol{R}_i$, that is, $\boldsymbol{r}_i=\boldsymbol{x}_i-\boldsymbol{R}_i$. The distance R between the monomers is defined by $R=|\boldsymbol{R}_1-\boldsymbol{R}_2|$.

leased energy is transferred to an adjacent monomer, mediated by virtual photon exchange, and an electron is ejected from $|\varphi_{\mathrm{ov}_2}\rangle$. The exchange term $V_{\mathrm{ov}_1,\mathrm{ov}_2,\boldsymbol{k},\mathrm{iv}}$, on the other hand, describes the transfer of an electron from a neighboring monomer into the innervalence hole. The subsequently emitted electron stems from the site of the initial ionization. Owing to the compactness of an innervalence orbital, the direct term dominates by far. There is hardly any overlap between $|\varphi_{\mathrm{iv}}\rangle$ and $|\varphi_{\mathrm{ov}_2}\rangle$. Therefore, ICD is characterized by energy transfer between neighboring monomers. Experimental evidence for such a process is available.[27,28] Note in passing that similar coupling matrix elements are encountered in Penning ionization.[29] There, however, it is electron transfer, and *not* energy transfer, which represents the underlying mechanism most appropriately.

How does $V_{\mathrm{ov}_1,\mathrm{ov}_2,\mathrm{iv},\boldsymbol{k}}$ depend on the distance R between the monomers involved in the decay? For the nearest neighbors in a cluster or a condensed matter system this is not easy to answer in general, for in this case there usually is a region between the two monomers where neither $|\varphi_{\mathrm{ov}_1}\rangle$ nor $|\varphi_{\mathrm{ov}_2}\rangle$ vanish. The spatial extension of each monomer is therefore not small in relation to R, thus rendering a power series expansion in $1/R$ not feasible. [A similar observation has led to the conclusion that in a covalently bound molecule interatomic contributions to the Auger decay of a core hole must not be neglected (see, for example, Ref. 30).] However, for the second and higher coordination shells of the monomer carrying the initial innervalence hole, a series expansion does make sense. Utilizing the expansion (for the employed notation please see Fig. 2)

$$\frac{1}{|\boldsymbol{x}_1-\boldsymbol{x}_2|}=\frac{1}{R}-\frac{\boldsymbol{u}_R\cdot(\boldsymbol{r}_1-\boldsymbol{r}_2)}{R^2}+\frac{3[\boldsymbol{u}_R\cdot(\boldsymbol{r}_1-\boldsymbol{r}_2)]^2-(\boldsymbol{r}_1-\boldsymbol{r}_2)^2}{2R^3}+O\left(\frac{1}{R^4}\right), \tag{18}$$

where $\boldsymbol{u}_R:=(\boldsymbol{R}_1-\boldsymbol{R}_2)/R$ is a unit vector along the line segment that joins the centers of mass, $\boldsymbol{R}_1$ and $\boldsymbol{R}_2$, of the two monomers under consideration, it is straightforward to obtain

$$V_{\mathrm{ov}_1,\mathrm{ov}_2,\mathrm{iv},\boldsymbol{k}}=\frac{1}{R^3}(\langle\varphi_{\mathrm{ov}_1}|e\boldsymbol{r}_1|\varphi_{\mathrm{iv}}\rangle\cdot\langle\varphi_{\mathrm{ov}_2}|e\boldsymbol{r}_2|\varphi_{\boldsymbol{k}}\rangle - 3\langle\varphi_{\mathrm{ov}_1}|e\boldsymbol{r}_1\cdot\boldsymbol{u}_R|\varphi_{\mathrm{iv}}\rangle\langle\varphi_{\mathrm{ov}_2}|e\boldsymbol{r}_2\cdot\boldsymbol{u}_R|\varphi_{\boldsymbol{k}}\rangle)+O\left(\frac{1}{R^4}\right). \tag{19}$$

Here we have exploited the fact that $\langle\varphi_{\mathrm{ov}_1}|\varphi_{\mathrm{iv}}\rangle=0=\langle\varphi_{\mathrm{ov}_2}|\varphi_{\boldsymbol{k}}\rangle$.

The leading term in Eq. (19) describes the interaction of two electric dipoles. According to Eqs. (17) and (19), the partial width corresponding to a single decay channel characterized by two outervalence holes—one being localized at the initially ionized monomer and another one at a monomer in the coordination shell of radius R of the former monomer—displays a $1/R^6$ dependence for sufficiently large R. Since the surface of a coordination shell, and therefore the number of monomers in this coordination shell, increases as R^2, the number of such decay channels depends, roughly, quadratically on R. Adding up all partial widths associated with a coordination shell of radius R, their total contribution to the ICD width Γ_{iv} decreases as $1/R^4$ as R is increased. If polarization effects of the medium inside the coordination shell are taken into account, the drop of Γ_{iv} as a function of R is likely to be even more pronounced. In view of these results, as soon as the first coordination shell is filled, the ICD width of a cationic innervalence state in a weakly bound cluster is expected to converge quickly as more and more monomers are added. We would like to mention that this behavior is in sharp contrast to the electronic decay rates of holes in the delocalized gas of valence electrons in metal clusters.[31] Pronounced electronic shell effects cause the lifetimes in these systems to be sensitively dependent on cluster size. The dependence is nonmonotonic, the lifetimes lying between a few femtoseconds and hundreds of nanoseconds.

The $1/R^6$ dependence of the energy transfer rate is known from Förster dipole-dipole coupling,[32] discussed in the context of electronic excitation energy transfer between a pair of chromophores.[33] There, all electronic states involved are bound and, for this reason, discrete. Energy conservation requires that the energy released by one chromophore can be resonantly absorbed by the other one. Usually this is possible only due to the involvement of nuclear motion, which therefore sets the time scale for the energy transfer process to picoseconds or longer. By contrast, in decay phenomena like ICD the energy transfer is associated with a transition to a continuum state, and energy conservation is fulfilled without any necessity for nuclear dynamics. One might argue that coupling matrix elements involving continuum electrons are very small, leading to rather long lifetimes. In ICD, however, the kinetic energy of a decay electron is just a few electronvolts. The corresponding de Broglie wavelength is of the order of 1 nm, which is comparable with the spatial extension of an atomic or molecular monomer in a cluster. Hence, the wave function of an ICD electron is relatively slowly oscillating and there are no pronounced cancellation effects that would lead to a small decay rate. Additionally, the low-

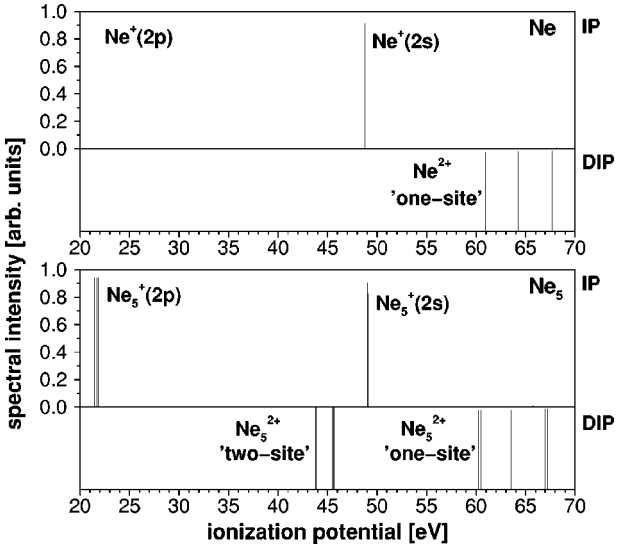

FIG. 3. Single (IP) and double (DIP) ionization potentials of Ne and Ne_5 in the valence regime. Note that in contrast to the isolated atom there are dicationic states of the cluster that are characterizable by a distribution of the two positive charges over at least two monomers (''two-site''). They are lower in energy than those monocationic states which arise from the removal of a $2s$ electron. In the cluster the $2s$-hole states can therefore undergo relaxation by electron emission. The corresponding cationic innervalence state of the isolated monomer, for which only ''one-site'' doubly ionized states exist, is stationary.

kinetic-energy nature of ICD electrons is the reason why a description using standard Gaussian basis sets augmented by a few diffuse functions—as presented in the ensuing section—is successful. None of the approximations typically employed for calculating Auger decay, which is associated with the emission of high-kinetic-energy electrons, are needed here.

III. SIZE DEPENDENCE OF ELECTRONIC DECAY RATE IN NEON CLUSTERS

In order to illustrate the general concepts described above, as well as to provide additional insight, we present in this section the results of *ab initio* calculations on neon clusters of different sizes. Neon clusters are a natural choice for such a prototype study. The interaction between the monomers is extremely weak. It is therefore possible to associate each innervalence orbital with an individual neon atom. Additionally, our new results extend in a systematic manner the work we carried out on Ne_2 and Ne_3.[15,34]

First we would like to show that innervalence ionized neon clusters can indeed decay by electron emission. In Fig. 3 single and double ionization spectra of the neon atom and, as a representative example of a neon cluster, Ne_5 are shown. The spectra were calculated within the framework of Green's function methods,[35] making use of the algebraic diagrammatic construction scheme (ADC).[36] ADC(n) represents a sophisticated perturbation theoretical approximation of a many-body Green's function, which is complete up to nth order and includes in addition infinite summations over certain classes of expansion contributions. The problem of finding the poles of a Green's function, which are directly related to observable quantities, is reformulated in terms of a Hermitian eigenvalue problem. This can be efficiently solved by a block-Lanczos approach.[37] The ADC method is ideally suited for the investigation of clusters because of its inherent size consistency.

The perturbation expansion underlying ADC is based on the partitioning $\hat{H}=\hat{F}+\hat{H}_I$ [see Eq. (2)], the Fock operator of N particles representing the unperturbed system. Thus, the orbital energies and Coulomb integrals obtained from Hartree-Fock calculations on the neutral ground state of Ne and Ne_5, respectively, serve as input for the ADC calculations. The Hartree-Fock calculations were performed with the *ab initio* program package GAMESS-UK.[38] We utilized the Gaussian basis set d-aug-cc-pVDZ (Ref. 39) for the single neon atom as well as the central atom in Ne_5, where the other four atoms, described by means of the basis set aug-cc-pVDZ,[39] are assumed to form a tetrahedron surrounding the central Ne atom. The distance between center and exterior atom was taken to be the interatomic equilibrium distance in solid neon, $R=3.13$ Å.[40] To describe single-electron removal we employed the ADC(3) approximation of the one-particle Green's function,[36] and to compute the double ionization spectra we used the ADC(2) scheme for the two-particle propagator.[41,42]

The spectral intensities in Fig. 3 do not immediately reflect the signal intensity in an experimental photoionization spectrum. We assume that the sudden approximation is valid, i.e., that the incident photon energy is larger by several electronvolts than the binding energy of the photoelectron. Under this assumption it is possible to use the spectral intensities given here and deduce from them photoemission probabilities.[43]

As can be seen in Fig. 3, the lowest double ionization energy of an isolated Ne atom is about 61 eV. This is much higher in energy than the cationic innervalence state, which according to our computations is located at about 48.5 eV, in agreement with experiment (see, for example, Ref. 44). An innervalence hole in an isolated neon monomer can therefore not decay by electron emission. In analogy to the single atom, dicationic *one-site* states, where both positive charges are localized at one monomer, exist in the cluster as well. However, in addition to these there are dicationic *two-site* states available in the cluster. The *two-site* states are lower in energy than the cationic innervalence states. Hence, in marked contrast to the single atom, the $2s$-hole states in the cluster are autoionizing resonances, i.e., discrete, quasibound states embedded in and interacting with an electronic continuum. The decay mechanism is ICD.

We have shown that electronic decay *can* take place. It is crucial to determine, in addition, the time scale on which ICD occurs and study how ICD lifetimes depend on cluster size. To that end we consider the clusters Ne_2, Ne_3, Ne_4, Ne_5, Ne_7, Ne_9, and Ne_{13}. The geometry of each Ne_n, except Ne_{13}, is constructed by adding to a central neon atom an environment of highest possible symmetry consisting of $n-1$ atoms at a distance of $R=3.13$ Å from the center. In Ne_{13} the 12 atoms surrounding the central neon atom are

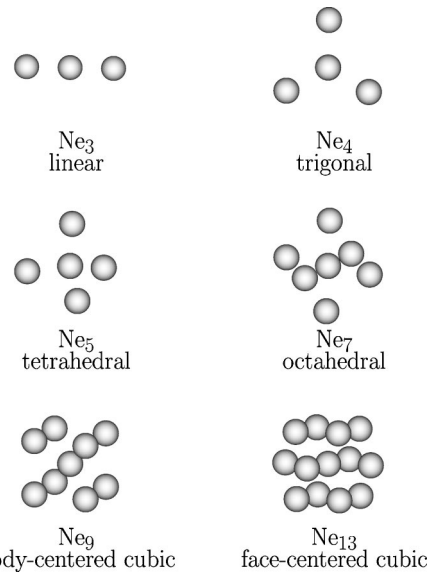

FIG. 4. Geometries of some selected neon clusters. In each cluster a central atom is surrounded by a coordination shell of radius $R=3.13$ Å. The structures are designed to converge to the complete first coordination shell of an atom in a neon crystal.

arranged in such a way to coincide with the complete first coordination shell in solid neon, which has a face-centered cubic crystal structure.[40] The resulting structures are shown in Fig. 4. The chosen geometries of the clusters do not represent minimum energy structures. They do, however, converge systematically towards the structure of solid neon.

In order to calculate the ICD lifetime of a $2s$ hole in the central neon atom we employed the spin-free version of Eq. (17):

$$\begin{aligned}\Gamma_{\mathrm{iv}} = 2\pi \sum_{\boldsymbol{k}} \sum_{\mathrm{ov}_1} \sum_{\mathrm{ov}_2 > \mathrm{ov}_1} & |V_{\mathrm{ov}_1,\mathrm{ov}_2[\mathrm{iv},\boldsymbol{k}]}|^2 \delta(\varepsilon_{\mathrm{iv}} - \varepsilon_{\mathrm{ov}_1} - \varepsilon_{\mathrm{ov}_2} \\ & + V_{\mathrm{ov}_1,\mathrm{ov}_2[\mathrm{ov}_1,\mathrm{ov}_2]} + \varepsilon_{\boldsymbol{k}} - V_{\boldsymbol{k},\mathrm{ov}_1[\boldsymbol{k},\mathrm{ov}_1]} - V_{\boldsymbol{k},\mathrm{ov}_2[\boldsymbol{k},\mathrm{ov}_2]}) \\ & + 2\pi \sum_{\boldsymbol{k}} \sum_{\mathrm{ov}_1} \sum_{\mathrm{ov}_2 > \mathrm{ov}_1} |V_{\mathrm{ov}_1,\mathrm{ov}_2,\mathrm{iv},\boldsymbol{k}}|^2 \delta(\varepsilon_{\mathrm{iv}} - \varepsilon_{\mathrm{ov}_1} - \varepsilon_{\mathrm{ov}_2} \\ & + V_{\mathrm{ov}_1,\mathrm{ov}_2,\mathrm{ov}_1,\mathrm{ov}_2} + \varepsilon_{\boldsymbol{k}} - V_{\boldsymbol{k},\mathrm{ov}_1,\boldsymbol{k},\mathrm{ov}_1} - V_{\boldsymbol{k},\mathrm{ov}_2[\boldsymbol{k},\mathrm{ov}_2]}) \\ & + 2\pi \sum_{\boldsymbol{k}} \sum_{\mathrm{ov}_1} \sum_{\mathrm{ov}_2 > \mathrm{ov}_1} |V_{\mathrm{ov}_1,\mathrm{ov}_2,\boldsymbol{k},\mathrm{iv}}|^2 \delta(\varepsilon_{\mathrm{iv}} - \varepsilon_{\mathrm{ov}_1} - \varepsilon_{\mathrm{ov}_2} \\ & + V_{\mathrm{ov}_1,\mathrm{ov}_2,\mathrm{ov}_1,\mathrm{ov}_2} + \varepsilon_{\boldsymbol{k}} - V_{\boldsymbol{k},\mathrm{ov}_1[\boldsymbol{k},\mathrm{ov}_1]} - V_{\boldsymbol{k},\mathrm{ov}_2,\boldsymbol{k},\mathrm{ov}_2}) \\ & + 2\pi \sum_{\boldsymbol{k}} \sum_{\mathrm{ov}_1} |V_{\mathrm{ov}_1,\mathrm{ov}_1,\mathrm{iv},\boldsymbol{k}}|^2 \delta(\varepsilon_{\mathrm{iv}} - 2\varepsilon_{\mathrm{ov}_1} \\ & + V_{\mathrm{ov}_1,\mathrm{ov}_1,\mathrm{ov}_1,\mathrm{ov}_1} + \varepsilon_{\boldsymbol{k}} - 2V_{\boldsymbol{k},\mathrm{ov}_1,\boldsymbol{k},\mathrm{ov}_1} + V_{\boldsymbol{k},\mathrm{ov}_1,\mathrm{ov}1,\boldsymbol{k}}). \end{aligned} \tag{20}$$

Please note that in this equation the spin degree-of-freedom is integrated out and all indices refer to *spatial* orbitals.

The quantities needed to evaluate Eq. (20) are orbital energies and certain Coulomb matrix elements in the spatial orbital basis. Using GAMESS-UK we calculated all matrix elements in the Gaussian basis set d-aug-cc-pVDZ and performed a Hartree-Fock self-consistent-field calculation on the neutral ground state of each cluster considered. In this way the orbital energies and the representation of the spatial orbitals in the Gaussian basis were obtained. For efficiency we implemented a *selective* transformation of the Coulomb matrix elements from the Gaussian to the spatial orbital basis, that is, we calculated only those matrix elements actually required. A complete transformation—the standard in current *ab initio* program packages—is prohibitively expensive for the larger neon clusters.

A direct evaluation of Eq. (20) is a delicate problem, because, as mentioned previously, the one-electron state $|\varphi_{\boldsymbol{k}}\rangle$ describing the emitted ICD electron is not square integrable. Continuum states are delta-function normalized:

$$\langle \varphi_{\boldsymbol{k}} | \varphi_{\boldsymbol{k}'} \rangle = \delta(\varepsilon_{\boldsymbol{k}} - \varepsilon_{\boldsymbol{k}'}). \tag{21}$$

Thus, at first glance it may seem that Hilbert space techniques, which are the basis of computational quantum mechanics, cannot be applied to calculating decay rates. However, this difficulty can be overcome by a computationally efficient method, the Stieltjes-Chebyshev moment-theory approach, discussed in detail in the literature.[45,46]

We first identify all accessible decay channels, i.e., all two-hole outervalence states that are lower in energy than the considered one-hole innervalence state. Practical *ab initio* calculations are performed in a finite basis set, and a finite number of discrete virtual orbitals $|\varphi_{\boldsymbol{k}_n}\rangle$ serve as approximations to continuum states. Hence, in a second step we determine for each individual decay channel $c_{\mathrm{ov}_1} c_{\mathrm{ov}_2} |\Phi_0^N\rangle$ the energy-dependent quantities

$$\Gamma_{\mathrm{ov}_1,\mathrm{ov}_2}(n) := 2\pi |V_{\mathrm{ov}_1,\mathrm{ov}_2[\mathrm{iv},\boldsymbol{k}_n]}|^2 \tag{22}$$

as well as the energies

$$\begin{aligned}\Delta E_{\mathrm{ov}_1,\mathrm{ov}_2}(n) := \varepsilon_{\mathrm{iv}} - \varepsilon_{\mathrm{ov}_1} - \varepsilon_{\mathrm{ov}_2} + V_{\mathrm{ov}_1,\mathrm{ov}_2[\mathrm{ov}_1,\mathrm{ov}_2]} + \varepsilon_{\boldsymbol{k}_n} \\ - V_{\boldsymbol{k}_n,\mathrm{ov}_1[\boldsymbol{k}_n,\mathrm{ov}_1]} - V_{\boldsymbol{k}_n,\mathrm{ov}_2[\boldsymbol{k}_n,\mathrm{ov}_2]}. \end{aligned} \tag{23}$$

[For the sake of clarity we have used the compact spin-orbital formulation of Eq. (17).] The discrete pseudospectrum $(\Delta E_{\mathrm{ov}_1,\mathrm{ov}_2}(n), \Gamma_{\mathrm{ov}_1,\mathrm{ov}_2}(n))$ is analyzed by making use of Stieltjes-Chebyshev moment theory. This technique allows one to extract the point $(0, \Gamma_{\mathrm{ov}_1,\mathrm{ov}_2})$ from the pseudospectrum, where $\Gamma_{\mathrm{ov}_1,\mathrm{ov}_2}$ is the partial decay width corresponding to channel $c_{\mathrm{ov}_1} c_{\mathrm{ov}_2} |\Phi_0^N\rangle$, incorporating proper normalization of the continuum.

The total ICD widths and the corresponding lifetimes are shown in Fig. 5. The most striking phenomenon that can be seen is the significant increase of Γ_{iv}, starting with a few meV in Ne_2—in agreement with studies performed using other theoretical techniques[15,34]—and going up to more than 200 meV in Ne_{13}. The lifetime in the latter is only about 3 fs. From the discussion in Sec. II the cause of this behavior is clear: In the larger clusters there are more interatomic decay channels available than in the smaller ones.

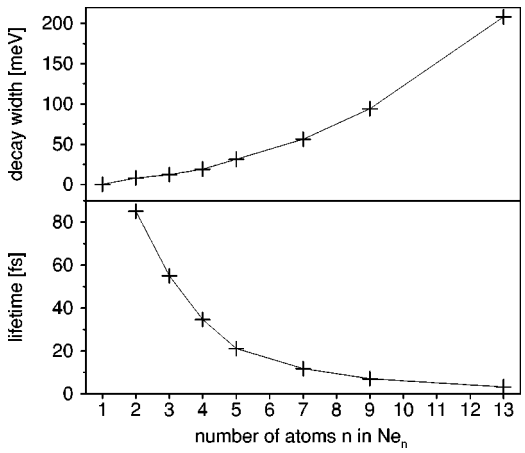

FIG. 5. Electronic decay width and corresponding lifetime of an innervalence ($2s$) hole in neon clusters of different sizes. The data were calculated by means of Eq. (20).

The number of relevant decay channels should be proportional to $n-1$, n being the number of atoms in the cluster, because for efficient coupling one of the final-state holes must be localized on the central neon atom. In fact, as a careful analysis of our numerical data has confirmed, decay channels with *both* final-state holes in the coordination shell of the central monomer do not give any appreciable contribution to Γ_{iv}. The coupling of the relevant decay channels to the innervalence hole state might be affected by the interatomic distances *within* the coordination shell—the distances of all shell atoms to the central atom are identical, but the distances between shell atoms decrease with increasing cluster size. The consequence would be a noticeable dependence of the average partial decay width on the number of atoms. This is one possible reason why the calculated ICD width is not linear as a function of cluster size (see Fig. 5). Another reason might be the quality of the Gaussian basis set used: the basis set improves with the size of the cluster. This implies that the description of the ICD electron is best for Ne_{13}.

By focusing on an innervalence hole on the central monomer we simulated the situation inside the solid. The ICD lifetime found in Ne_{13} is a restrictive upper bound for the ICD lifetime of a $2s$ hole in a neon crystal. For surface atoms, which do not possess a complete coordination shell of nearest neighbors, our data suggest that the ICD lifetime is of the order of 10 fs.

In principle the innervalence ionized cluster can give off its excess energy by photon emission. The fluorescence decay width of an innervalence excited Ne atom is of the order of 1 μeV (see Ref. 47, and references therein). That quantity is expected to be of similar magnitude in a neon cluster. We have shown that ICD is faster by at least three orders of magnitude than relaxation by photon emission, which may therefore be neglected. In Ne_2, nuclear dynamics and ICD take place on comparable time scales, giving rise to interesting dynamical effects accompanying ICD.[15,34] However, in view of the ultrashort lifetimes found in the larger neon clusters, it is very likely that for these systems ICD is the fastest process occurring.

IV. SUGGESTIONS FOR EXPERIMENTS

Based on our work it seems likely that intermolecular Coulombic decay of innervalence vacancies plays an important role in the huge class of weakly bound clusters and condensed matter, comprising such systems as water, carbon dioxide, and ethanole. If energy conservation allows ICD to take place, it is expected to dominate the relaxation of innervalence holes. The only competing processes typically occur on a longer time scale. The kinetic energy distribution of the ICD electrons extends from 0 up to several electronvolts. Its detailed structure depends on the available electronic decay channels and on effects induced by the motion of the atomic nuclei, which we have found to make a particularly pronounced impact due to the Coulomb repulsion acting in the dicationic final state.[15,34] From these considerations it is evident that ICD deserves attention.

A simple experimental approach to ICD is suggested by the results of the previous section. One could sort the clusters according to size and measure, with a high resolution, the spectral line of the innervalence photoelectron for each cluster size. While the line position is insensitive to cluster size (see, for example, Fig. 3), the width is expected to be size dependent (Fig. 5). Pursuing this strategy is, presumably, not too difficult, but the wealth of information the ICD effect contains cannot be revealed in this way. To that end a measurement of the kinetic energy distribution of the ICD electron is needed.

There are, however, a few obstacles to observing ICD electrons in a routine experiment. First, electron spectroscopy in the energy range of a few electronvolts is more problematic than for faster electrons. This is a technical difficulty, and experimentalists certainly are making progress in this direction. The second problem is somewhat more fundamental. In order to investigate the decay of an innervalence hole one would expose a given system to photons whose energy is sufficient to produce such a vacancy. Obviously, for systems that can undergo ICD this photon energy is above the double ionization threshold. Thus it may happen that an absorbed photon simultaneously ejects two outervalence electrons, instead of ionizing an innervalence electron that is followed, in a second step, by the spontaneous emission of an ICD electron.

The emission of correlated electron pairs from the surface of a solid following one-photon absorption has been investigated experimentally by Biester and co-workers[26] and by Herrmann *et al.*,[48] and within a theoretical approach by Berakdar.[49] With the restriction of energy conservation, the energy of each of the electrons in a correlated pair can take on any value between 0 and E_{max}, which is the energy of the absorbed photon minus the double ionization potential of the generated dication. The two correlated electrons share the total energy available to them, E_{max}, in a complementary fashion, that is, if one of the electrons has kinetic energy ε, the other one has kinetic energy $E_{\mathrm{max}}-\varepsilon$. The corresponding continuous spectrum, which can be influenced by varying the photon energy, may interfere with the measurement of the kinetic energy distribution of the ICD electrons.

The question now is how electrons stemming from two-

electron photoemission can be cleanly distinguished from ICD electrons or even avoided. One possible strategy is rooted in the observation that an innervalence photoelectron arises at fixed binding energy and an ICD electron at fixed kinetic energy, i.e., both quantities are independent of photon energy. Thus, after the innervalence peak has been identified, the kinetic energy distribution of all electrons that are detected in coincidence with the innervalence photoelectron is measured at several photon energies. This procedure should, in principle, allow an unambiguous identification of ICD electrons and their spectrum.

A second, probably more effective technique consists in removing an outervalence electron first. The photon energy needed to achieve this can be chosen significantly below the double ionization threshold, and ionization of the outervalence shell is rather efficient. Then, by tuning the photon energy appropriately, one can resonantly excite an innervalence electron into the outervalence hole. The cross section for this second step is also large, provided that the outervalence hole is not completely delocalized. In cationic neon clusters, for example, the described approach should work well, because in the ground state the positive charge is restricted to basically two atoms.[50] As soon as the photon energy is in resonance with the innervalence-outervalence transition, the slow ICD electrons emerge from the surface of the investigated system. This serves as an observable signature of the energy transfer from the resonantly excited cationic monomer to its neighbors.

The second of the two proposed realizations of dedicated ICD experiments is reminiscent of *multiatom resonant photoemission* (MARPE) discovered in core-excitation studies of metal oxides.[51,52] In a MARPE experiment, a specific atomic species is resonantly core excited. If the corresponding excitation energy is large enough, the excited atom can relax by ionizing a core electron of a neighboring atom. This electron is detected. Because both the excitation energy and the core ionization potential are characteristic of the involved atomic species, MARPE promises to become an important analytical tool. Though similar in principle, the most striking difference to ICD is that autoionization of the initially core-excited atom is much more likely than energy transfer to a neighbor, whereas practically *all* innervalence excited cationic monomers in a cluster are expected to decay via ICD, since all other electronic decay channels are closed. Another difference is the relevance of retardation effects. They are negligible in the energy regime of valence levels, but of importance to understanding energy transfer in core-excitation experiments (see Ref. 52, and references therein).

An intriguing possibility is the use of free-electron lasers[53–55] for ICD experiments. Their intense and coherent radiation could be employed for ionizing the outervalence shell of the sample and exciting the innervalence-outervalence transition by two-photon absorption. Performing such an experiment on Ne_2, for instance, would require photons with an energy of about 27.5 eV, creating outervalence electrons of roughly 6 eV and ICD electrons distributed between 0 and 3 eV.[15,34]

In this paper we have presented an elementary theoretical description of ICD and applied it to investigate the behavior of the intermolecular Coulombic decay rate of an innervalence ionized monomer as a function of the number of its nearest neighbors. As the size of the system is increased, more and more decay channels are opened. We have shown that the electronic decay rate is extremely short in the larger systems, of the order of 1 fs in Ne_{13}^+. ICD is an ultrafast process, in particular in extended systems. Its time scale is comparable with that one familiar from the Auger decay of core holes. Therefore, detecting ICD in condensed matter systems which consist of weakly bound molecules appears to be possible. In fact, a probably higher signal rate in comparison to clusters should simplify the measurement of the kinetic energy spectrum of the ICD electrons. It may turn out that the ICD phenomenon discovered in clusters is an ideal tool for investigating intermolecular interactions in condensed matter. We hope that our work will stimulate experiments.

ACKNOWLEDGMENTS

We would like to thank Thomas Sommerfeld for helpful discussions. Partial support by the Deutsche Forschungsgemeinschaft is acknowledged.

[1] Science **271**, 920 (1996), Special issue on clusters.
[2] *Van der Waals Molecules II*, edited by J. Michl, Chem. Rev. **94** (American Chemical Society, 1994).
[3] S. Sugano and H. Koizumi, *Microcluster Physics* (Springer, Berlin, 1998).
[4] S. Hüfner, *Photoelectron Spectroscopy* (Springer, Berlin, 1996).
[5] N.V. Dobrodey, A.I. Streltsov, and L.S. Cederbaum, Chem. Phys. Lett. **339**, 263 (2001).
[6] M. Thompson, M.D. Baker, A. Christie, and J.F. Tyson, *Auger Electron Spectroscopy* (Wiley, New York, 1985).
[7] T.X. Carroll, J. Hahne, T.D. Thomas, L.J. Sæthre, N. Berrah, J. Bozek, and E. Kukk, Phys. Rev. A **61**, 042503 (2000).
[8] R. Flesch, A.A. Pavlychev, J.J. Neville, J. Blumberg, M. Kuhlmann, W. Tappe, F. Senf, O. Schwarzkopf, A.P. Hitchcock, and E. Rühl, Phys. Rev. Lett. **86**, 3767 (2001).
[9] L.S. Cederbaum, J. Zobeley, and F. Tarantelli, Phys. Rev. Lett. **79**, 4778 (1997).
[10] J. Zobeley, L.S. Cederbaum, and F. Tarantelli, J. Chem. Phys. **108**, 9737 (1998).
[11] J. Zobeley, L.S. Cederbaum, and F. Tarantelli, J. Phys. Chem. A **103**, 11 145 (1999).
[12] R. Santra, J. Breidbach, J. Zobeley, and L.S. Cederbaum, J. Chem. Phys. **112**, 9243 (2000).
[13] R. Santra, L.S. Cederbaum, and H.-D. Meyer, Chem. Phys. Lett. **303**, 413 (1999).
[14] R. Santra, J. Zobeley, L.S. Cederbaum, and F. Tarantelli, J. Electron Spectrosc. Relat. Phenom. **114-116**, 41 (2001).
[15] R. Santra, J. Zobeley, L.S. Cederbaum, and N. Moiseyev, Phys.

Rev. Lett. **85**, 4490 (2000).
[16] G.A. Sawatzky, Phys. Rev. Lett. **39**, 504 (1977).
[17] T.D. Thomas and P. Weightman, Chem. Phys. Lett. **81**, 325 (1981).
[18] O. Madelung, *Introduction to Solid-State Theory* (Springer, Berlin, 1978).
[19] A. Szabo and N. S. Ostlund, *Modern Quantum Chemistry* (Dover, Mineola, 1996).
[20] A.L. Fetter and J.D. Walecka, *Quantum Theory of Many-Particle Systems* (McGraw-Hill, Boston, 1971).
[21] J.J. Sakurai, *Modern Quantum Mechanics* (Addison-Wesley, Reading, 1994).
[22] T. Koopmans, Physica (Amsterdam) **1**, 104 (1933).
[23] L.S. Cederbaum, W. Domcke, J. Schirmer, and W. von Niessen, Adv. Chem. Phys. **65**, 115 (1986).
[24] V.F. Weisskopf and E.P. Wigner, Z. Phys. **63**, 54 (1930).
[25] E. Rühl, C. Schmale, H.C. Schmelz, and H. Baumgärtel, Chem. Phys. Lett. **191**, 430 (1992).
[26] H.W. Biester, M.J. Besnard, G. Dujardin, L. Hellner, and E.E. Koch, Phys. Rev. Lett. **59**, 1277 (1987).
[27] R. Thissen, P. Lablanquie, R.I. Hall, M. Ukai, and K. Ito, Eur. Phys. J. D **4**, 335 (1998).
[28] U. Hergenhahn, A. Kolmakov, O. Löfken, M. Riedler, A. R. B. de Castro, and T. Möller (unpublished).
[29] P.E. Siska, Rev. Mod. Phys. **65**, 337 (1993).
[30] H. Wormeester, H.J. Borg, and A. van Silfhout, Surf. Sci. **258**, 197 (1991).
[31] M.E. Garcia, Ll. Serra, F. Garcias, and K.H. Bennemann, Phys. Rev. B **57**, 4895 (1998).
[32] T. Förster, Ann. Phys. (Leipzig) **6**, 55 (1948).
[33] T. Renger, V. May, and O. Kühn, Phys. Rep. **343**, 137 (2001).
[34] N. Moiseyev, R. Santra, J. Zobeley, and L.S. Cederbaum, J. Chem. Phys. **114**, 7351 (2001).
[35] L.S. Cederbaum, in *Encyclopedia of Computational Chemistry*, edited by P. v. R. Schleyer (Wiley, New York, 1998).
[36] J. Schirmer, L.S. Cederbaum, and O. Walter, Phys. Rev. A **28**, 1237 (1983).
[37] H.-G. Weikert, H.-D. Meyer, L.S. Cederbaum, and F. Tarantelli, J. Chem. Phys. **104**, 7122 (1996).
[38] GAMESS-UK is a package of *ab initio* programs written by M.F. Guest, J.H. van Lenthe, J. Kendrick, K. Schoffel, and P. Sherwood, with contributions from R.D. Amos, R.J. Buenker, H.J.J. van Dam, M. Dupuis, N.C. Handy, I.H. Hillier, P.J. Knowles, V. Bonacic-Koutecky, W. von Niessen, R.J. Harrison, A.P. Rendell, V.R. Saunders, A.J. Stone, and A.H. de Vries. The package is derived from the original GAMESS code due to M. Dupuis, D. Spangler and J. Wendoloski, NRCC Software Catalog, Vol. 1, Program No. QG01 (GAMESS), 1980.
[39] T.H. Dunning, Jr., J. Chem. Phys. **90**, 1007 (1989); R.A. Kendall, T.H. Dunning, Jr., and R.J. Harrison, *ibid.* **96**, 6796 (1992); D.E. Woon and T.H. Dunning, Jr., *ibid.* **100**, 2975 (1994); Basis sets were obtained from the Extensible Computational Chemistry Environment Basis Set Database, Version 1.0, as developed and distributed by the Molecular Science Computing Facility, Environmental and Molecular Sciences Laboratory which is part of the Pacific Northwest Laboratory, P.O. Box 999, Richland, Washington 99352, USA, and funded by the U.S. Department of Energy. The Pacific Northwest Laboratory is a multi-program laboratory operated by Battelle Memorial Institue for the U.S. Department of Energy under Contract No. DE-AC06-76RLO 1830.
[40] D.G. Henshaw, Phys. Rev. **111**, 1470 (1958).
[41] J. Schirmer and A. Barth, Z. Phys. A **317**, 267 (1984).
[42] F.O. Gottfried, L.S. Cederbaum, and F. Tarantelli, Phys. Rev. A **53**, 2118 (1996).
[43] L.S. Cederbaum and W. Domcke, Adv. Chem. Phys. **36**, 205 (1977).
[44] O. Wilhelmi, G. Mentzel, B. Zimmermann, K.-H. Schartner, H. Schmoranzer, F. Vollweiler, S. Lauer, and H. Liebel, J. Electron Spectrosc. Relat. Phenom. **101-103**, 155 (1999).
[45] P.W. Langhoff, in *Electron-Molecule and Photon-Molecule Collisions*, edited by T. Rescigno, V. McKoy, and B. Schneider (Plenum Press, New York, 1979).
[46] A.U. Hazi, in *Electron-Molecule and Photon-Molecule Collisions* (Ref. 45).
[47] P. Lablanquie, F. Penent, R.I. Hall, J.H.D. Eland, P. Bolognesi, D. Cooper, G.C. King, L. Avaldi, R. Camilloni, S. Stranges, M. Coreno, K.C. Prince, A. Müehleisen, and M. Žitnik, Phys. Rev. Lett. **84**, 431 (2000).
[48] R. Herrmann, S. Samarin, H. Schwabe, and J. Kirschner, Phys. Rev. Lett. **81**, 2148 (1998).
[49] J. Berakdar, Phys. Rev. B **58**, 9808 (1998).
[50] F.Y. Naumkin and D.J. Wales, Mol. Phys. **93**, 633 (1998).
[51] A.W. Kay, E. Arenholz, B.S. Mun, F.J. Garcia de Abajo, C.S. Fadley, R. Denecke, Z. Hussain, and M.A. Van Hove, Science **281**, 679 (1998).
[52] A.W. Kay, F.J. Garcia de Abajo, S.-H. Yang, E. Arenholz, B.S. Mun, N. Mannella, Z. Hussain, M.A. Van Hove, and C.S. Fadley, J. Electron Spectrosc. Relat. Phenom. **114-116**, 1179 (2001).
[53] C. Pagani, E.L. Saldin, E.A. Schneidmiller, and M.V. Yurkov, Nucl. Instrum. Methods Phys. Res. A **423**, 190 (1999).
[54] H.P. Freund and G.R. Neil, Proc. IEEE **87**, 782 (1999).
[55] T. Möller, J. Alloys Compd. **286**, 1 (1999).